$= 3.8 \times 10^5\ s^{-1}$, based on correction of the LFP carbene decay data (method 1) for competing dimerization, and $E_a = 7.4$ kcal/mol, $\log A = 11.1\ s^{-1}$. This affords $\Delta G^{\ddagger} \sim 9.8$ kcal/mol, $\Delta H^{\ddagger} \sim 6.8$ kcal/mol, and $\Delta S^{\ddagger} \sim -10$ eu. Note that our previously reported parameters, based on ab initio molecular orbital calculations, are $\Delta G^{\ddagger} = 9.0$ kcal/mol, $\Delta H^{\ddagger} = 8.2$ kcal/mol, and $\Delta S^{\ddagger} = -2.7$ eu.[10]

The important difference between our results and those of Liu and Bonneau lies in *the relative roles of enthalpy and entropy*. Both laboratories, using experimental and computational approaches, arrive at very similar $\Delta G^{\ddagger}$ values (9-10 kcal/mol), but the apportionment between $\Delta H^{\ddagger}$ and $\Delta S^{\ddagger}$ varies greatly. Whereas we now find $\Delta S^{\ddagger}$ to be principally responsible for the "slow" CyCCl → **2** rearrangement, Liu and Bonneau and our electronic structure calculations implicate a "high" E_a ($\Delta H^{\ddagger}$). However, the present E_a and $\log A$ values are confirmed by four independent sets of measurements, and we observe no complications due to dimerization. Accordingly, we suggest that $\Delta H^{\ddagger} \sim 2.5$ kcal/mol and $\Delta S^{\ddagger} \sim -20$ eu represent a more accurate picture of the CyCCl → **2** isomerization process.[18]

Why is the unimolecular rearrangement of CyCCl, driven by ~50 kcal/mol in ΔG_{rx},[10] opposed by such an unfavorable entropy? The experimental determination of activation parameters characterizes a statistical ensemble of carbene molecules in solution, whereas the computed values reflect properties of two stationary points on the potential energy surface of an isolated carbene in the gas phase. The very different values obtained imply that significant differences exist between the energy surfaces. One possibility is that the variational transition state of the reaction (corresponding to the maximum on the $\Delta G^{\ddagger}$ profile) does not coincide with the calculated conventional minimum energy transition state.[19] In a reaction that crosses a relatively flat potential energy surface (low E_a),[2,19] entropic control may become particularly important. Interestingly, a detailed computational analysis of the concerted rearrangement of CyCH to cyclobutene reveals a very intricate, correlated set of atomic motions between the migrating methylene and carbenic carbons.[20] Should analogous behavior occur in the CyCCl → **2** isomerization, it could contribute to the unfavorable $\Delta S^{\ddagger}$. Furthermore, the migrating group is always "anchored" to the other methylene carbon in the ring, and this may also restrict the ease of travel across the barrier. The pass over the energy barrier would be very narrow with steep side walls due to the unusual constraints imposed on the transition state by the required changes in bonding and geometry. Many energetically favorable collisions will not be effective in channelling the energy into motion along the reaction coordinate through the pass, hence a large negative entropy of activation will be measured.[21] This effect must be dynamic in origin because an entropic change of -20 eu in an isolated molecule as small as CyCCl during a 1,2 shift is inconceivable. The large negative entropy of activation indicates that the reaction must have a transmission coefficient that is significantly less than unity. Extensive theoretical explorations of the reaction surfaces will be essential for a clearer understanding of intramolecular carbenic rearrangements.

Acknowledgments. We are grateful to the National Science Foundation (R.A.M.) and to the donors of the Petroleum Research Fund, administered by the American Chemical Society (K.K.-J.), for financial support. We thank Professors R. S. Sheridan and M. A. Cotter for helpful discussions.

Supplementary Material Available: Tables of rate constants and temperatures for the Arrhenius correlations of methods 1-4 (3 pages). Ordering information is given on any current masthead page.

(18) Indeed, the 1,2 hydride shift of CH_3CCl to vinyl chloride ($k \sim 1.3 \times 10^6\ s^{-1}$) appears to be governed by $E_a \sim 4.9$ kcal/mol ($\Delta H^{\ddagger} \sim 4.3$ kcal/mol), $\log A = 9.7\ s^{-1}$ ($\Delta S^{\ddagger} \sim -16$ eu), and hence $\Delta G^{\ddagger} \sim 8.1$ kcal/mol, consistent with "a highly ordered transition state."[6] Molecular orbital calculations on CH_3CCl (analogous to those presented in ref 10 for CyCCl) give $\Delta H^{\ddagger} = 11.4$ kcal/mol, $\Delta S^{\ddagger} = -2.2$ eu, and thus $\Delta G^{\ddagger} = 12.4$ kcal/mol at $T = 300$ K.

(19) Blake, J. F.; Wierschke, S. G.; Jorgensen, W. L. *J. Am. Chem. Soc.* **1989**, *111*, 1919. See also: Houk, K. N.; Rondan, N. G.; Mareda, J., ref 2.

(20) Wang, R.; Deng, C. *Tetrahedron* **1988**, *44*, 7335. See also: Shevlin, P. B.; McKee, M. L. *J. Am. Chem. Soc.* **1989**, *111*, 519.

(21) This viewpoint is analogous to the introduction of the empirical "steric" factor ($P = A_{obsd}/A_{calcd}$) in simple collision theory to account for the fraction of energetically suitable bimolecular collisions that also have the proper geometric orientation. The ratio of computed to measured $\Delta S^{\ddagger}$ is ~7, corresponding to a correction factor (or a transmission coefficient) of $\sim 10^{-3}$.

Transmembrane Electron Transfer Catalyzed by Phospholipid-Linked Manganese Porphyrins

Mamoru Nango,* Atsushi Mizusawa, Takenori Miyake, and Junji Yoshinaga†

Department of Applied Chemistry
College of Engineering
University of Osaka Prefecture
Sakai, Osaka 591, Japan
Sawai Pharmaceutical Co. Ltd.
Asahi-ku, Osaka 535, Japan
Received July 10, 1989

Synthetic models can be very helpful in studying the effect of distance and orientation in electron transfer reactions in biological membrane processes such as occur in photosynthesis and mitochondoria.[1-3] To provide a model for the electron transfer where porphyrin pigments play the key role, the preparation of porphyrin derivatives that are capable of light-induced intra- or intermolecular electron transfer was reported.[3] However, there has been little study of ground-state electron transfer between porphyrin complexes to provide insight into the effect of distance and orientation in the electron transfer so that a vectorial electron transfer system may be constructed in the biological membrane.[4-8] We now report transmembrane electron transfer catalyzed by manganese complexes of bilayer-active phospholipid-linked porphyrins **1**, PE-C_n-MnTTP ($n = 0, 5, 11$) (Scheme I), which can be easily immersed into the lipid bilayer. The synthetic procedures leading to compound **1** are described in the following sequence of steps. The porphyrins 5-[4-[[(5-carboxyalkyl)amino]carbonyl]-phenyl]-10,15,20-tri-*p*-tolylporphyrin, TTPCONH$(CH_2)_n$*COOH*, **2** ($n = 0, 5, 11$), and their manganese complexes, Mn(III)-TTPCONH$(CH_2)_n$*COOH*, **3**, were synthesized as described in an earlier paper.[6] Either **2** or **3** was treated with ethyl chloroformate in chloroform at low temperature and reacted with dipalmitoylphosphatidylethanolamine (DPPE) overnight to give the phospholipid-linked porphyrin PE-C_n-MTTP (yields 60-70%), followed by chromatographic separation (silica gel, 10% acetone–chloroform).[9] The ^1H NMR and mass spectra of PE-C_n-TTP support unambiguously the assigned structure. The chemical shifts of NMR spectra for all peaks were as expected.[9] MS spectra of PE-C_n-TTP indicated one porphyrin per phospholipid. The absorption spectra of PE-C_n-MTTP in CH_2Cl_2–10% EtOH and phospholipid vesicles such as egg yolk phosphatidylcholine (egg PC, Nippon Fine Chemical Co.) and dipalmitoylphosphatidylcholine (DPPC, Nippon Fine Chemical Co.) were identical, and all showed the presence of a normal porphyrin chromophore. No change of these absorption spectra of PE-C_n-TTP and PE-C_n-

† Sawai Pharmaceutical Co. Ltd.

(1) Govindjee, Ed. *Photosynthesis*; Academic Press: New York, 1982; Vol. 1.

(2) Clayton, R. K., Sistrom, W. R., Eds. *The Photosynthetic Bacteria*; Plenum Press: New York, 1978.

(3) Barber, J., Ed. *Topics in Photosynthesis*; Elsevier/North-Holland Biochemical Press: New York, 1979; Vol. 3.

(4) Tabushi, I.; Nishiya, T.; Shimomura, M.; Kunitake, T.; Inokuchi, H.; Yagi, T. *J. Am. Chem. Soc.* **1984**, *106*, 219-226.

(5) Dannhauser, T.; Nango, M.; Oku, N.; Anzai, K.; Loach, P. A. *J. Am. Chem. Soc.* **1986**, *108*, 5865.

(6) Nango, M.; Dannhauser, T.; Huang, D.; Spears, K.; Morrison, L.; Loach, P. A. *Macromolecules* **1984**, *17*, 1898.

(7) Nango, M.; Kryu, H.; Loach, P. A. *J. Chem. Soc., Chem. Commun.* **1988**, 697-698.

(8) Runquist, J. A.; Loach, P. A. *Biochem. Biophys. Acta* **1981**, *637*, 231.

(9) A more detailed synthetic method and analytical data will be reported elsewhere.

0002-7863/90/1512-1640$02.50/0

Scheme I. Phospholipid-Linked Porphyrins (PE-C_n-MTTP)

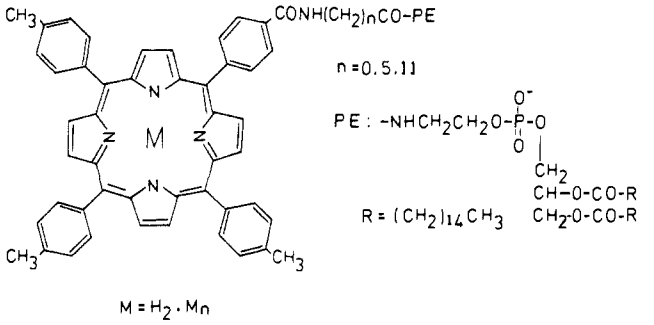

MnTTP in egg PC or DPPC vesicle was observed upon increasing their concentration from 2.5 to 50 nmol/10 mg lipid, suggesting no aggregation of the porphyrins in the lipid vesicle. Relative fluorescence intensities for PE-C_{11}-TTP in several media at 25 °C showed that higher fluorescence yields were observed in DPPC vesicle and egg PC vesicle, 138 and 130, respectively, where the values were normalized to yields in CH_2Cl_2–10% EtOH which were set at 100. Similar results were obtained for the other phospholipid-linked porphyrins, PE-TTP and PE-C_5-TTP. The data, therefore, imply that in the vesicle systems the porphyrin moiety is immersed within the hydrophobic interior of the membrane. To further examine the interaction of the PE-linked porphyrin complexes with the lipid bilayer, we attempted to remove the PE-linked porphyrin complexes from the external vesicle surface by gel filtration.[6] The visible spectra of the vesicles were measured before and after gel filtration indicated that the porphyrin portion of PE-MnTTP was almost completely bound to either egg PC vesicle or DPPC vesicles, up to the concentration 100 or 50 nmol/10 mg lipid, depending upon the vesicle. Similar results were obtained for the other phospholipid-linked porphyrins, PE-C_5-MnTTP and PE-C_{11}-MnTTP. The maximum incorporation of the porphyrin into the vesicle was higher by almost 5–10 times than MnTTP. These data, again, imply that in the vesicle systems the porphyrin moiety is easily incorporated into the hydrophobic interior of the membrane.

Electron transfer from an external reductant (reduced indigotetrasulfonic acid, $ITSAH_2$, 1×10^{-5} M) to potassium ferricyanide (0.1 M) trapped within a phospholipid liposome (either egg PC or DPPC) was measured anaerobically at 0.4 M imidazole buffer at pH = 7.0 as mediated by a catalyst of PE-linked manganese porphyrins incorporated in the vesicle bilayer.[5,8]

Figure 1 illustrates the rate of electron transport (V_0) across egg PC liposomes at 25 °C with increased complex concentration and across DPPC liposomes at various temperatures. As is apparent from Figure 1, PE-MnTTP showed little or no catalytic activity in both vesicle systems. In contrast, both PE-C_5-MnTTP and PE-C_{11}-MnTTP catalyzed transmembrane electron transport in egg PC vesicle (Figure 1a) and above 40 °C (near phase transition, T_c) in DPPC vesicle (Figure 1b). Significantly enhanced electron transfer was observed for PE-C_{11}-MnTTP compared to PE-C_5-MnTTP. Furthermore, as is apparent from Figure 1b, PE-C_5-MnTTP and PE-C_{11}-MnTTP exhibited two regions of enhanced electron transfer near 33 and above 42 °C where the temperature is probably near the pretransition and T_c of the lipid, respectively.[10,11] In contrast, all PE-C_n-MnTTP showed little or no catalytic activity below the phase transition of DPPC liposome. Thus, it appears that only when the temperature is near either the pretransition or the main phase transition are PE-C_5-MnTTP and PE-C_{11}-MnTTP sufficiently mobile to catalyze electron transport, reasonably related to the melting of the phospholipid bilayer.[12] Our result is the first example of electron transport

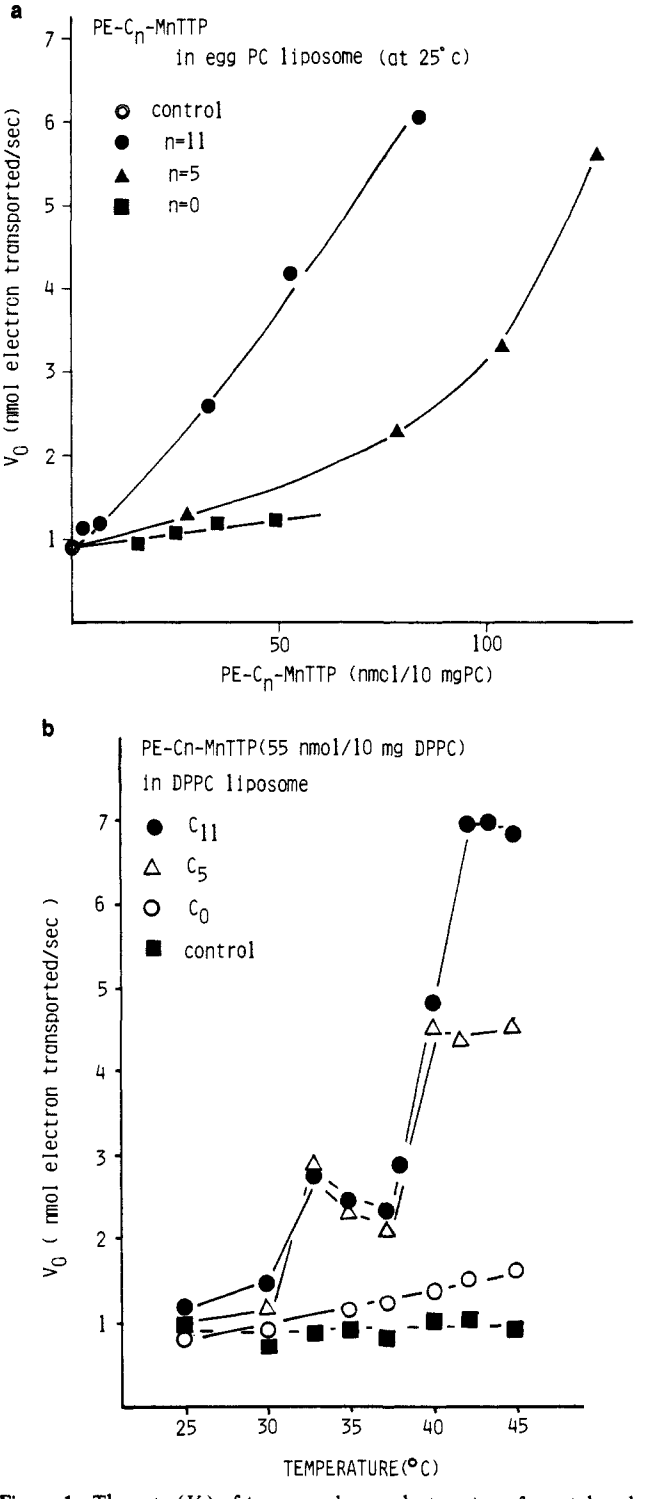

Figure 1. The rate (V_0) of transmembrane electron transfer catalyzed by PE-C_n-MnTTP (n = 0, 5, 11) (a) as a function of porphyrin concentration in egg yolk PC vesicle at 25 °C and (b) in DPPC vesicle at various temperatures.

that occurred at both pretransition and phase transition temperatures of liposomal membrane, reflecting the gel–liquid transformation of the lipid bilayer. Interestingly, MnTTP showed enhanced electron transfer in DPPC vesicle only when the temperature was above the main phase transition of the lipid (data not shown). Thus, it is likely that the electron transport catalyzed by PE-C_n-MnTTP correlates easily with transformation of the lipid bilayer. The mechanism of electron transfer catalyzed by PE-C_5-MnTTP and PE-C_{11}-MnTTP is presumed to follow a similar pathway which manganese complexes of poly(ethylenimine)-linked tetratolylporphyrins, PEI-C_{11}-MnTTP, catalyzed, as illustrated previously.[5] That is, electron transfer from this

(10) Jain, M. K., Wagner, R. C., Eds. *Introduction to Biological Membranes*; John Wiley and Sons: New York, 1980.
(11) Fendler, J. H., Ed. *Membrane Mimetic Chemistry*; John Wiley and Sons: New York, 1982.
(12) Tabushi, I.; Hamachi, I.; Kobuke, Y. *Tetrahedron Lett.* **1987**, *28*, 5899–5902.

manganous porphyrin to a manganic porphyrin tethered to a PE molecule on the opposite side of the bilayer can occur. We have assumed that the PE-linked porphyrins can penetrate into the membrane up to the phosphoric acid head group of the lipid and the distance these porphyrins penetrate into the lipid bilayer should be different with different PE-C_n-TTP (n = 0, 5, 11). It is likely that this is the reason why PE-C_{11}-MnTTP and PE-C_5-MnTTP can catalyze the electron transfer more than PE-MnTTP (Figure 1) because the MnTTP portion of the C_{11} and C_5 derivatives can approach each other sufficiently for electron transfer to occur.[5]

In conclusion, these results showed that (1) PE-C_n-MnTTP exhibited a selective transmembrane electron transfer, depending not only on the length of spacer methylene groups of PE-C_n-MnTTP incorporated in the lipsome but also on the fluidity of the lipid bilayer and (2) **1** can be embedded into the lipid bilayer of liposome much more easily than MnTTP. Thus, these compounds are being utilized to systematically examine electron transport in selected liposomal systems.

Acknowledgment. M.N. thanks Prof. P. A. Loach, Northwestern University, for helpful discussions.

Planar "20-Electron" Osmium Imido Complexes. A Linear Imido Ligand Does Not Necessarily Donate Its Lone Pair of Electrons to the Metal

J. T. Anhaus, T. P. Kee, M. H. Schofield, and R. R. Schrock*

Department of Chemistry 6-331
Massachusetts Institute of Technology
Cambridge, Massachusetts 02139
Received September 6, 1989

We have been using the (2,6-diisopropylphenyl)imido ligand as a stabilizing ligand for high-oxidation-state Mo alkylidene,[1] W alkylidene,[2] Re alkylidene,[3] and Re alkylidyne[4] complexes. In order to explore the potential of a similar approach to the high-oxidation-state organometallic chemistry of later metals, and in view of the relative scarcity of imido complexes of group 8 and 9 metals,[5] we have begun to explore the preparation and chemistry of new imido complexes of osmium, the metal that yielded the first example of a transition-metal imido complex, Os(N-*t*-Bu)O_3.[6]

OsO_4 reacts with 3 equiv of ArNCO (Ar = 2,6-C_6H_3-*i*-Pr_2) smoothly over the course of ~20 h in refluxing heptane to afford deep red-brown, crystalline Os(N-2,6-C_6H_3-*i*-$Pr_2)_3$ (**1**) in 50% isolated yield.[7] An X-ray study[8] shows **1** to be a planar trigonal complex (Figure 1) in which a crystallographic 2-fold axis passes through Os, N(2), C(21), and C(24). Two of the phenyl rings are oriented roughly perpendicular to the OsN_3 plane (dihedral angle 81.62°), while the third lies in the OsN_3 plane (dihedral angle 1.90°). The two crystallographically distinct imido ligands are linear (Os-N(1)-C(11) = 178.0 (5)°, Os-N(2)-C(21) = 180° by symmetry). If we assume imido ligand linearity to indicate that the lone pair of electrons on nitrogen is donated to the metal, **1** is a "20-electron" complex. In D_{3h} symmetry, one can construct σ-bonding metal orbitals from s, p_x, and p_y orbitals, and five π-bonding metal orbitals, three using combinations of p_z (a_2''), d_{xz}, and d_{yz} (e'') and two using combinations of $d_{x^2-y^2}$ and d_{xy} (e') orbitals. Two electrons are left in the d_{z^2} (a_1') orbital on osmium, and the last remaining pair of electrons we propose is located in a nitrogen-centered nonbonding MO of a_2' symmetry made up of the "in-plane" p_x orbitals on the nitrogen atoms.[9] SCF-Xα-SW calculations on hypothetical $Os(NH)_3$ suggest that the HOMO is the metal-based a_1' (d_{z^2}) orbital, the ligand-based a_2' orbital being approximately 1 eV lower in energy.[10]

^{1}H and ^{13}C NMR data[11] indicate that all three imido ligands are equivalent in **1** in CD_2Cl_2 between 25 and -90 °C. Therefore

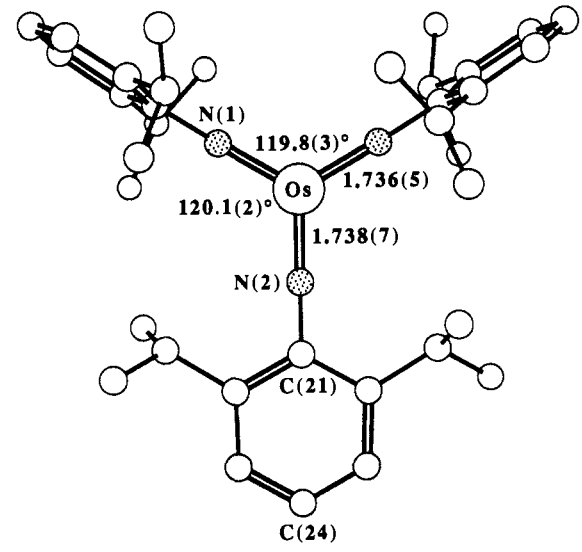

Figure 1. A drawing of the structure of Os(N-2,6-C_6H_3-*i*-$Pr_2)_3$. (Only "covalent" Os=N bonds are shown.)

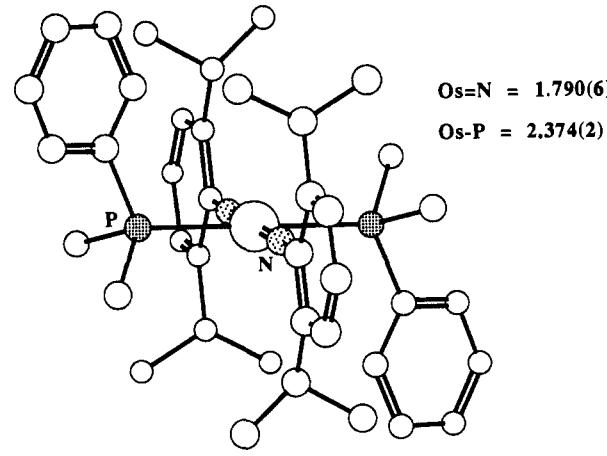

Figure 2. A drawing of *trans*-Os(N-2,6-C_6H_3-*i*-$Pr_2)_2(PMe_2Ph)_2$.

(1) (a) Murdzek, J. S.; Schrock, R. R. *Organometallics* **1987**, *6*, 1373. (b) Schrock, R. R.; Murdzek, J. S.; Bazan, G.; Robbins, J.; DiMare, M.; O'Regan, M. *J. Am. Chem. Soc.*, in press.

(2) Schrock, R. R.; DePue, R.; Feldman, J.; Schaverien, C. J.; Dewan, J. C.; Liu, A. H. *J. Am. Chem. Soc.* **1988**, *110*, 1423.

(3) Horton, A. D.; Schrock, R. R. *Polyhedron* **1988**, *7*, 1841.

(4) Schrock, R. R.; Weinstock, I. A.; Horton, A. D.; Liu, A. H.; Schofield, M. H. *J. Am. Chem. Soc.* **1988**, *110*, 2686.

(5) Nugent, W. A.; Mayer, J. M. *Metal-Ligand Multiple Bonds*; Wiley and Sons: New York, 1988.

(6) (a) Clifford, A. F.; Kobayashi, C. S. *Abstracts of Papers*, 130th National Meeting of the American Chemical Society, Atlantic City, NJ; American Chemical Society, Washington, DC, 1956; p 50R. (b) Clifford, A. F.; Kobayashi, C. S. *Inorg. Synth.* **1960**, *6*, 207.

(7) A solution of OsO_4 (2.0 g, 7.87 mmol) and ArNCO (4.8 g, 23.65 mmol) in heptane (40 mL) was refluxed under argon for 20 h, during which time the initial yellow solution became a dark brown. Red-brown crystals of **1** precipitated from solution upon cooling of the reaction mixture to -35 °C for ~2 h. The crude product was recrystallized from pentane (-35 °C) to obtain pure **1** in 50% yield. Anal. Calcd for $C_{36}H_{51}N_3Os$: C, 60.39; H, 7.18; N, 5.87. Found: C, 60.60; H, 7.22; N, 5.77.

(8) A crystal was mounted on a glass fiber in air. Data were collected on an Enraf-Nonius CAD-4 diffractometer at room temperature using Mo Kα radiation: space group $C2/c$ with a = 22.616 (2) Å, b = 10.2831 (4) Å, c = 16.185 (1) Å, β = 111.462 (6)°, Z = 4, FW = 716.02, and ρ = 1.357 g/cm^3. A total of 4291 reflections ($h,k,\pm l$) were collected in the range 3° < 2θ < 55° with the 2824 having $I > 3.00\sigma(I)$ being used in the structure refinement by full-matrix least-squares techniques (180 variables) using the TEXSAN crystallographic software package from Molecular Structure Corporation. Final R_1 = 0.042, R_2 = 0.041. Full details can be found in the supplementary material.

(9) (a) There are other examples of occupied "ligand nonbonding" or "peripheral" orbitals.[9b,c] (b) Chu, S.-Y.; Hoffmann, R. *J. Phys. Chem.* **1982**, *86*, 1289. (c) Laine, R. M.; Moriarty, R. E.; Bau, R. *J. Am. Chem. Soc.* **1972**, *94*, 1402.

(10) Schofield, M.; Johnson, K., unpublished results. Full details will be published in the full paper.

(11) ^{1}H NMR (C_6D_6): δ 7.33 (H_p), 7.03 (H_m), 3.84 (Me_2CH), 1.21 (Me_2CH). ^{13}C NMR (C_6D_6): δ 155.67 (C_{ipso}), 139.51 (C_o), 128.25 (C_m), 123.30 (C_p), 29.08 (Me_2CH), 22.92 (Me_2CH).

0002-7863/90/1512-1642$02.50/0